Magnetic and electronic structures of antiferromagnetic $La_2NiO_{4+ delta}$ and $La_{2-x}Sr_xNiO_{4+ delta}$: ^{139}La nuclear quadrupole resonance study

1993 J. Phys.: Condens. Matter 5 765

(http://iopscience.iop.org/0953-8984/5/7/005)

J. Phys.: Condens. Matter 5 (1993) 765–780. Printed in the UK

Magnetic and electronic structures of antiferromagnetic $La_2NiO_{4+\delta}$ and $La_{2-x}Sr_xNiO_{4+\delta}$: ^{139}La nuclear quadrupole resonance study

Shinji Wada†, Yuji Furukawa†, Makoto Kaburagi†, Tsuyoshi Kajitani‡, Syoichi Hosoya‡ and Yoshihiro Yamada§

† College of Liberal Arts, Kobe University, Nada, Kobe 657, Japan
‡ Institute for Materials Research, Tohoku University, Sendai 980, Japan
§ Himeji Institute of Technology, Shyosya, Himeji 671-22, Japan

Received 18 May 1992, in final form 25 September 1992

Abstract. We carried out a nuclear quadrupole resonance study of ^{139}La in $La_{2-x}Sr_xNiO_{4+\delta}$ ($\delta = 0.00$–0.10; $x = 0.0$–1.3) in the temperature range $T = 1.4$–200 K, paying particular attention to its relationship to the superconducting cuprates. In lanthanum nickel oxide, the occupation of holes on both Ni $3d_{x^2-y^2}$ and $3d_{z^2}$ orbitals with parallel spins ($S = 1$) causes some characteristic properties.

(1) The large internal magnetic field ($H_{int} = 26$–18 kOe) at the La site indicates the existence of a strong transferred exchange interaction between Ni $3d_{z^2}$ and La 6s orbitals through the $2p_z$ orbital of apex oxygen.

(2) Discontinuities in the magnitude of H_{int} and electric field gradient observed at $\delta \simeq 0.02$ are attributed to the crystal phase transition from a low-T orthorhombic to a high-T tetragonal phase.

(3) Up to high Sr doping (close to the phase transition at $x \simeq 1.0$ from antiferromagnetic to paramagnetic), H_{int} remains almost constant, suggesting that the doped holes first go into the $3d_{x^2-y^2}$ orbital without producing Ni–Ni spin frustrations.

(4) The T dependences of H_{int} and relaxation rate T_1^{-1} at low T are explained basically by the spin-wave theory for three-dimensional antiferromagnets, and the sublattice magnetic moments of Ni^{2+} are close to the localized spins.

(5) The dependence of T_1^{-1} proportional to $T^{2.6}$ indicates that the ^{139}La relaxation can be attributed to the short-wavelength antiferromagnetic fluctuations notwithstanding the geometrical cancellation at the La site.

1. Introduction

Recently some characteristic properties shown by the layered perovskites La_2MO_4 (M ≡ Cu, Ni, Co), such as the metal–semiconductor and structural phase transitions, and antiferromagnetic (AF) ordering, have been the subject of great interest in helping to investigate the mechanisms of *high-T_c* superconductivity appearing in $(La, Sr)_2CuO_4$ solid solutions.

In the case of La_2CuO_4, the configuration of Cu^{2+} is d^9 and one hole of the Cu ion occupies the $3d_{x^2-y^2}$ orbital which is strongly hybridized with the $2p_x$ and $2p_y$ orbitals of Cu–O planar oxygen. Then the evolution from the AF to the superconducting and to the normal metallic state when one introduces excess holes by Sr atom substitution

for the La atom has been studied extensively, with the main interest focused on the variation in the magnetic and electronic properties in the Cu–O plane.

Interest has also grown in the properties of the related compound La_2NiO_4. In this case, the configuration of Ni^{2+} is d^8, and both the $3d_{x^2-y^2}$ and the $3d_{z^2}$ orbitals are occupied by approximately one hole each, with parallel spins. This implies that the holes are also distributed on the $2p_z$ orbital of apex oxygen (O_{apex}) which is hybridized with the Ni $3d_{z^2}$ orbital and also with the La 6s orbital. One may therefore expect strong coupling between the Ni–O and La–O planes, and the electronic and magnetic properties of La_2NiO_4 would be affected not only by the planar oxygen (O_{planar}) atom as in the cuprates but also by the O_{apex} atom. It has been established that a stoichiometric sample of La_2NiO_4 is an electrical insulator and antiferromagnet with a Néel temperature $T_N \simeq 650$ K [1] and exhibits structural phase transitions from a high-temperature tetragonal (HTT) phase to a low-temperature orthorhombic (LTO_1) phase at about 700 K [2,3] and to a second low-temperature orthorhombic (LTO_2) phase at about 75 K [4,5].

An La_2NiO_4 crystal can accommodate excess oxygen up to $\delta \simeq 0.2$ in the interstitial positions of the La–O plane [6]. The deviation δ from the oxygen stoichiometry has been shown to decrease T_N [1,7,8] and the structural phase transition temperature [9]. In the case of $La_2CuO_{4+\delta}$, a small amount of excess oxygen destroys the AF ordering and produces partially a synthetic superconductor [10,11]. However, in the case of $La_2NiO_{4+\delta}$, the magnetic ordering persists up to large values of δ.

On the other hand, the substitution of Sr for La in the $La_{2-x}Sr_xNiO_{4+\delta}$ system leads to a metallic conductor, but more slowly than in the cuprates. The magnetic susceptibility and electric resistivity measurements made by Cava *et al* [12] suggested the existence of the conductive phase in the high-Sr-substitution range $x = 1.0$–1.4, with no sign of superconductivity. Recently, a ^{139}La nuclear magnetic resonance (NMR) study by Furukawa and Wada [13] provided microscopic evidence for the phase transition from the AF to the paramagnetic (metallic) state at $x \simeq 1$.

In this study, we focus our attention on the magnetic and electronic structures in the AF state of La_2NiO_4 and their changes when the holes are doped by the introduction of excess oxygen and also by the substitution of Sr. The static and dynamic properties of the magnetic moments and the electric field gradient (EFG) are probed through their influences on the ^{139}La spectrum of the nuclear quadrupole resonance (NQR) and on the temperature dependence of the spin–lattice relaxation time T_1, respectively. Preliminary results of the ^{139}La NQR study for powder samples of $La_2NiO_{4+\delta}$ ($\delta = 0.02$–0.1) were reported in our previous papers [14,15].

2. Samples

2.1. *Sample preparation*

As-sintered samples of $La_2NiO_{4+\delta}$ ($\delta \simeq 0.7$) were synthesized by the solid state reaction technique in air. Deoxygenated ($\delta = 0.0$, 0.2, 0.4) and oxygenated ($\delta = 1.0$) samples were obtained by annealing the as-sintered sample in high vacuum or in an O_2 gas atmosphere, respectively, for an appropriate number of days as described in our previous paper [14].

The stoichiometric sample of $La_2NiO_{4.00}$ prepared by annealing in a high vacuum at 800 °C for a month was a brown material and stable for more than a year under normal storage conditions.

A single crystal of $La_2NiO_{4.02}$ with dimensions of about 2 mm (along the c axis) × 2.5 mm × 5 mm was prepared to investigate the direction of the internal magnetic field H_{int} and the principal axis of the EFG with respect to the crystal axes. Details of the single-crystal growth and determination of the oxygen content were given by Kajitani *et al* [9].

2.2. *X-ray diffraction*

X-ray powder diffraction patterns were obtained using Cu Kα radiation. The dependences of the lattice parameters on δ at room temperature are shown in figure 1, where open, full and half-filled circles denote the c, a and b lattice parameters, respectively. The stoichiometric sample $La_2NiO_{4.00}$ was in the LTO_1 phase at room temperature and showed a phase transition from LTO_1 to LTO_2 at about 75 K. The $La_2NiO_{4.02}$ sample was also in the LTO_1 phase at room temperature, but the difference between the lattice parameters a and b was very small. On the other hand, the oxygenated samples of $La_2NiO_{4.07}$ and $La_2NiO_{4.10}$ were in the HTT phase at room temperature. These results agree with other studies, i.e. the transition temperature from HTT to LTO_1 phase decreases on increase in δ. As can be seen in the figure, the small increase in δ results in a significant increase in the c (*long-axis*) lattice parameter as reported by Gopalan *et al* [8].

The dependence of the lattice parameters on the Sr substitution content x is also plotted in figure 1. Open and full triangles denote the lattice parameters c and a (b), respectively. For $x < 0.5$, the unit cell stretches along the c axis and shrinks along the a and b axes. In the highly doped region ($x > 0.5$), the variations are reversed.

2.3. *Magnetic susceptibilities*

The magnetic susceptibility χ of the powder samples was measured in the temperature range $T = 4.2$–300 K using a torsion-type magnetic balance at 10 kOe. χ for the oxygen stoichiometric $La_2NiO_{4.00}$ was almost independent of T, while χ for all the non-stoichiometric samples ($\delta = 0.02$–0.10) increased with decreasing T as shown in figure 2. For $La_2NiO_{4.02}$, χ shows a broad cusp at around 170 K and a sharp peak at about 20 K. With the increase in excess oxygen content δ, both the cusp and the peak in $\chi(T)$ move towards lower temperatures. For $La_2NiO_{4.10}$, the broad cusp can be seen at about 45 K but the sharp peak is not observed down to 4.2 K.

3. ^{139}La magnetic resonance

3.1. *^{139}La resonance spectrum in $La_2NiO_{4+\delta}$ at 4.2 K and $H_{ext} = 0$*

A phase-coherent pulsed-NMR spectrometer was utilized for the measurements of the ^{139}La resonance spectrum and spin–lattice relaxation time T_1.

Figure 3 shows typical ^{139}La ($I = \frac{7}{2}$) spectra in $La_2NiO_{4+\delta}$ with $\delta = 0.00$, 0.02 and 0.10 at 4.2 K under the zero external magnetic field $H_{ext} = 0$. A small increase in δ leads to a drastic change in the resonance spectrum.

The main resonance lines can be analysed as a spectrum originating from the La sites where the Zeeman interaction is larger than the quadrupole interaction,

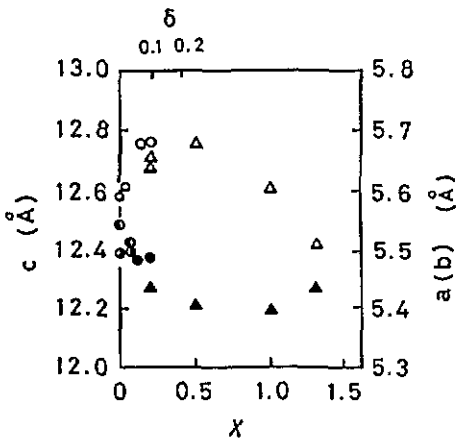

Figure 1. Dependence of lattice parameters on δ (○, ●, ○) and on x (△, ▲) at room temperature: ○, △, lattice parameter c; ●, ▲, lattice parameters $a(=b)$ in the tetragonal phase; ○, lattice parameters a and b in the orthorhombic phase.

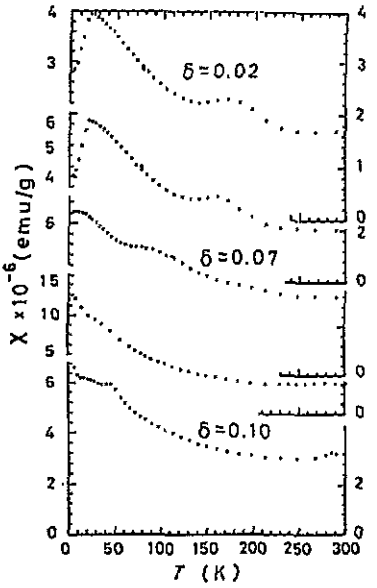

Figure 2. Temperature dependence of the magnetic susceptibility under an external field of 10 kOe for various non-stoichiometric $La_2NiO_{4+\delta}$ samples ($\delta = 0.02$–0.10).

$H_M \gg H_Q$, as discussed in the previous papers [14,15]. H_M and H_Q are expressed by [16]

$$H_Q = \tfrac{1}{6}h\nu_Q[3I_z^2 - I(I+1) + \tfrac{1}{2}\eta(I_+^2 + I_-^2)] \tag{1}$$

$$H_M = -\gamma_N \hbar \boldsymbol{H}_{int} \cdot \boldsymbol{I} \tag{2}$$

where $\nu_Q = \frac{3}{2}e^2qQ/2I(I+1)h$, $eq = V_{zz}$, $\boldsymbol{H}_{int}$ is the internal magnetic field at a polar angle θ with respect to the principal axis of V_{zz} and $\eta = (V_{xx} - V_{yy})/V_{zz}$ is the asymmetry parameter of the EFG. We assume here that $|V_{zz}| > |V_{yy}| > |V_{xx}|$.

For $\delta = 0.00$, one can separate the experimental lines into two groups composed of nearly equally separated lines. In the case of the group of lines shaded in figure 3(a) (hereafter denoted La(I)), the resonance position of the main peaks can be reproduced by equations (1) and (2) with the set of parameters

$$\nu_Q = 8.7 \text{ MHz} \qquad H_{int} = 26.2 \text{ kOe} \qquad \theta \simeq 77° \qquad \eta \simeq 0. \tag{3}$$

The other group of lines in figure 3(a) (denoted La(II)) is almost the same as that observed in $La_2NiO_{4.02}$ shown in figure 3(b).

For $\delta = 0.02$, we obtain the set of parameters

$$\nu_Q = 4.0 \text{ MHz} \qquad H_{int} = 18.3 \text{ kOe} \qquad \theta \simeq 77° \qquad \eta \simeq 0 \tag{4}$$

which reproduce the main peak positions [17].

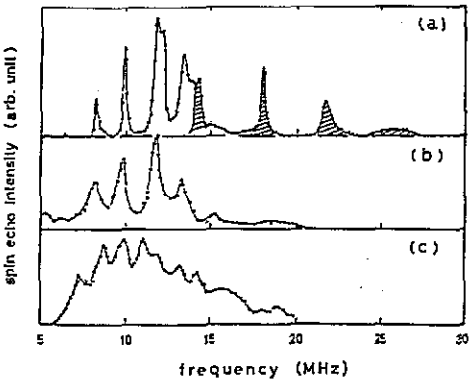

Figure 3. Typical ^{139}La ($I = \frac{7}{2}$) spectra in $La_2NiO_{4+\delta}$ at 4.2 K under a zero external magnetic field: (*a*) $\delta = 0.00$; (*b*) $\delta = 0.02$; (*c*) $\delta = 0.10$.

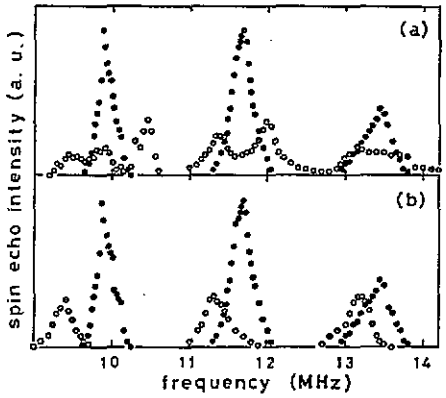

Figure 4. Central three lines associated with the transitions $|\frac{1}{2}\rangle \leftrightarrow |-\frac{1}{2}\rangle$ and $|\pm\frac{1}{2}\rangle \leftrightarrow |\pm\frac{3}{2}\rangle$ at 4.2 K for $H_{ext} = 0$ (●) and $H_{ext} = 5$ kOe (○): (*a*) H_{ext} along ⟨110⟩; (*b*) H_{ext} along ⟨001⟩.

For $\delta = 0.10$, the resonance lines shown in figure 3(*c*) are not well separated from each other. However, seven very distinguishable peaks in the spectrum are reproduced by the set of parameters

$$\nu_Q = 2.6 \text{ MHz} \qquad H_{int} = 17.8 \text{ kOe} \qquad \theta \simeq 78^\circ \qquad \eta \simeq 0. \tag{5}$$

It should be noted that the positions of the other small resonance peaks appearing in figure 3(*c*) agree with those of the main peaks in $La_2NiO_{4.02}$.

3.2. Dependence of the resonance spectrum on H_{ext} for a single crystal ($\delta = 0.02$)

In order to determine the direction of H_{int} with respect to the crystal axes, we investigated the ^{139}La NQR spectrum in the $La_2NiO_{4.02}$ single crystal under the external magnetic field H_{ext}. The Hamiltonian is given by

$$H = H_Q - \gamma_N \hbar \boldsymbol{I} \cdot (\boldsymbol{H}_{int} + \boldsymbol{H}_{ext}) \tag{6}$$

and, therefore, the ^{139}La spectrum should depend on the direction of H_{ext} with respect to the crystal axes.

Figure 4 shows the three resonance lines corresponding to the transitions $|\frac{1}{2}\rangle \leftrightarrow |-\frac{1}{2}\rangle$ and $|\pm\frac{1}{2}\rangle \leftrightarrow |\pm\frac{3}{2}\rangle$ at 4.2 K when $H_{ext} = 0$ (full circles) and $H_{ext} = 5$ kOe (open circles). H_{ext} is in the direction along the axis of ⟨110⟩ in figure 4(*a*) and ⟨001⟩ in figure 4(*b*). Here the lattice parameters are expressed by the tetragonal symmetry representation. The results are summarized as follows.

(1) When H_{ext} is in the direction parallel to ⟨110⟩, each line splits into two lines.

(2) When H_{ext} is in the direction perpendicular to ⟨110⟩, each line shifts towards lower frequencies.

(3) The magnitude of the frequency shift, approximately equal to ±0.10 MHz kOe^{-1} in both H_{ext} directions, is very small in comparison with the value of $\gamma_N = 0.601$ MHz kOe^{-1} for ^{139}La.

In the unit cell of La_2NiO_4, there are two La–O planes between the Ni–O planes. Then the directions of H_{int} at the La sites caused by the Ni moment are parallel and antiparallel in each plane along the axis of AF order. When H_{ext} is in the direction along the axis in which the Ni magnetic moments are ordered, the local field is given by $H_{int} \pm H_{ext}$, resulting in line splitting. On the other hand, H_{ext} in the direction perpendicular to the axis of the magnetic ordering merely shifts the resonance frequency. Thus the experimental results indicate the direction of the Ni magnetic moments to be along ⟨110⟩ in the basal Ni–O plane.

3.3. *Temperature dependence of the ^{139}La resonance spectrum*

Figure 5 shows a typical temperature dependence of the central lines for the $La_2NiO_{4.02}$ powder sample. Each main resonance line moves towards lower frequencies with increase in T, indicating a reduction in H_{int}. Below about 25 K, the main lines exhibit severe broadening. As the susceptibility $\chi(T)$ of $La_2NiO_{4.02}$ shows a sharp peak at about 20 K, this line broadening suggests the existence of magnetic ordering below about 20 K.

$\nu_M(T)/\nu_M(0)$ of the $|\frac{1}{2}\rangle \leftrightarrow |-\frac{1}{2}\rangle$ transition is plotted in figure 6. $\nu_M(T)/\nu_M(0)$ of La(I) in $La_2NiO_{4.00}$ (open triangles) shows a discontinuous increase at about 80 K and then a monotonic decrease at higher T. The discontinuity in $\nu_M(T)/\nu_M(0)$ must closely link to the structural transition from LTO_1 to LTO_2 at about 75 K found in the stoichiometric sample.

$\nu_M(T)/\nu_M(0)$ of La(II) in $La_2NiO_{4.00}$ (open circles) and La in $La_2NiO_{4.02}$ (full circles) decreases monotonically with the same reduction rate. For La in $La_2NiO_{4.10}$ (open squares), the reduction rate is the largest of all. This is consistent with the fact that T_N for the oxygenated sample is lower than for the deoxygenated sample.

In figure 5, one can see some weak and broad resonance lines moving towards lower frequencies on increase in T from about 77 K to about 150 K. The reduction rate of the resonance frequency with increasing T is larger than that of the main lines. Above about 170 K, these spurious resonance lines disappear. As $\chi(T)$ for $La_2NiO_{4.02}$ shows a broad cusp at about 170 K, these spurious lines probably originate from ^{139}La in a possible but small fraction of a magnetic phase with $T_N \simeq 170$ K.

As shown in figure 7, the quadrupole frequency ν_Q for ^{139}La in $La_2NiO_{4.02}$ exhibits a monotonic decrease on increase in T, similar to $\nu_Q(T)$ for ^{139}La in La_2CuO_4 [18].

3.4. *^{139}La spin–lattice relaxation time T_1 in $La_2NiO_{4+\delta}$*

A saturation recovery method was used to measure T_1 at the peak intensity point of the central line. In the case of ^{139}La ($I = \frac{7}{2}$), the spectrum is composed of seven almost equally separated lines, and the recovery curve of the magnetization $M(T)$ after the initial saturation between the $|\frac{1}{2}\rangle \leftrightarrow |-\frac{1}{2}\rangle$ transition levels is characterized by four time constants as [19]

$$[M(\infty) - M(t)]/M(\infty) = a_1 \exp(-2Wt) + a_2 \exp(-12Wt) + a_3 \exp(-30Wt) + a_4 \exp(-56Wt) \quad (7)$$

where $2W = T_1^{-1}$ and the a_i are the coefficients depending on the initial population of the $2I + 1$ nuclear spin levels imposed by the saturation RF pulses. We applied a $\pi/2$ RF pulse as the saturation pulse which provides the coefficients a_i as

$$a_1 = 0.013 \qquad a_2 = 0.068 \qquad a_3 = 0.206 \qquad a_4 = 0.714. \quad (8)$$

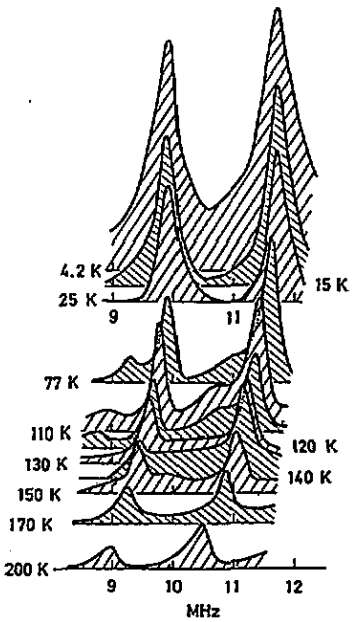

Figure 5. Typical temperature dependence of the central lines in the $La_2NiO_{4.02}$ powder sample.

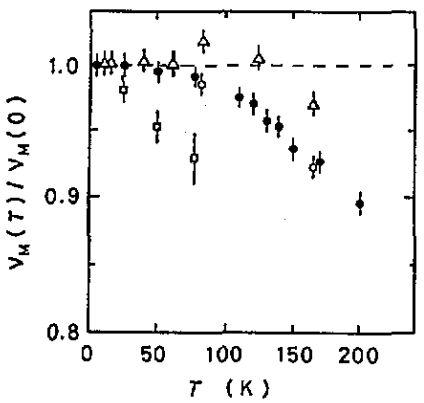

Figure 6. $\nu_M(T)/\nu_M(0)$ of the $|\frac{1}{2}\rangle \leftrightarrow |-\frac{1}{2}\rangle$ transition: Δ, La(I) sites in $La_2NiO_{4.00}$; ○, La(II) sites in $La_2NiO_{4.00}$; ●, La in $La_2NiO_{4.02}$; □, La in $La_2NiO_{4.10}$.

Figure 8 shows the typical experimental recovery curves of ^{139}La in the $La_2NiO_{4.02}$ powder at 1.4 and at 110 K. At high temperatures above about 140 K equations (7) and (8) could reproduce the experimental recovery curve. On decreasing T, however, a slowly recovering component grew and the fit of the data to equation (7) was unsuccessful. Then we tentatively assumed that the observed recovery curve was composed of two components with a slow relaxation rate $2W_L = (T_1^L)^{-1}$ and fast relaxation rate $2W_S = (T_1^S)^{-1}$. We carried out a fit using the following equation:

$$\begin{aligned}(M(\infty) - M(t)]/M(\infty) = M_L[a_1 \exp(-2W_L t) + a_2 \exp(-12W_L t) \\ + a_3 \exp(-30W_L t) + a_4 \exp(-56W_L t)] + M_S[a_1 \exp(-2W_S t) \\ + a_2 \exp(-12W_S t) + a_3 \exp(-30W_S t) + a_4 \exp(-56W_S t)] \qquad (9)\end{aligned}$$

where $M_L + M_S = 1$ and M_S was taken to be a free parameter giving the content of the fast relaxation component. A typical result of this analysis for $La_2NiO_{4.02}$ is shown in figure 9. As shown in the inset to the figure, $M_S = \frac{1}{2}$ at low T starts to increase above about 30 K and becomes unity above about 130 K. $(T_1^S)^{-1}$ and $(T_1^L)^{-1}$ show the same T dependence below about 60 K, indicating that they can be attributed to the same mechanism of relaxation.

The temperature dependence of T_1^{-1} for samples with $\delta = 0.00$, 0.02 and 0.10 are summarized in figure 10, where the triangles denote T_1^{-1} at the La(I) site in

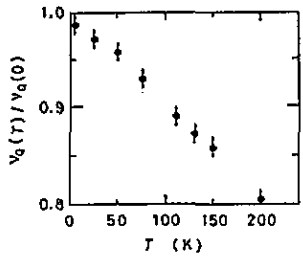

Figure 7. Temperature dependence of ν_Q at the La site in $La_2NiO_{4.02}$.

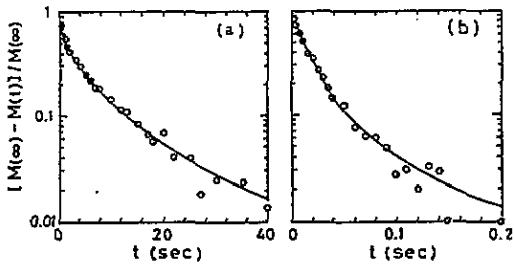

Figure 8. Experimental recovery curve of the longitudinal magnetization observed at the central resonance line of the $La_2NiO_{4.02}$ powder at (*a*) 1.4 K and (*b*) 110 K. ——, recovery curve obtained through the procedure described in the text.

$La_2NiO_{4.00}$, the circles denote T_1^{-1} at the La site in $La_2NiO_{4.02}$ and the squares denote T_1^{-1} at the La site in $La_2NiO_{4.10}$. The open and full symbols correspond to $(T_1^S)^{-1}$ and $(T_1^L)^{-1}$, respectively. T_1^{-1} for the La(II) site in $La_2NiO_{4.00}$ was exactly the same as that in $La_2NiO_{4.02}$ in both its magnitude and its dependence on T.

All the T_1^{-1}-values for $\delta < 0.02$ show almost the same temperature dependence below about 60 K; that is, T_1^{-1} increases in proportion to $T^{2.6}$ below about 20 K and shows a broad bump at about 40 K. On the other hand, T_1^{-1} for the oxygenated $La_2NiO_{4.10}$ sample is large and almost independent of T above 4.2 K.

Finally, for La(II) in $La_2NiO_{4.00}$, we can see that the magnitudes and the T dependences of H_{int}, ν_Q and T_1^{-1} are exactly the same as those in $La_2NiO_{4.02}$. Thus we conclude that the La(II) site observed fractionally in $La_2NiO_{4.00}$ is exactly the same as the dominant La site in $La_2NiO_{4.02}$.

3.5. ^{139}*La transverse relaxation time* T_2 *in* $La_2NiO_{4.02}$

The transverse relaxation time T_2 is determined by the decay curve as

$$M(2\tau) = M(0)\exp(-2\tau/T_2) \tag{10}$$

where $M(2\tau)$ is the intensity of the spin echo focused at 2τ after the application of $\pi/2$–π RF pulses separated by the time τ.

Above about 100 K, $M(2\tau)$ for $La_2NiO_{4.02}$ showed a single-exponential decay. On decreasing T, however, a slow decay component grew and the fit of the data to equation (10) was unsuccessful. Then we again assumed the observed decay curve to be composed of two components with a slow relaxation time T_2^L and a fast relaxation time T_2^S. Then we carried out a fit by the equation

$$M(2\tau) = M_S\exp(-2\tau/T_2^S) + M_L\exp(-2\tau/T_2^L) \tag{11}$$

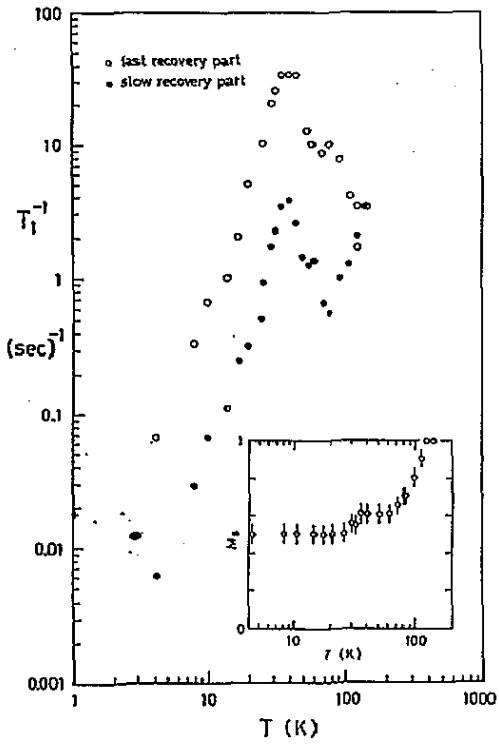

Figure 9. Temperature dependences of $(T_1^S)^{-1}$ and $(T_1^L)^{-1}$ of ^{139}La in $La_2NiO_{4.02}$. The inset shows the temperature dependence of M_S, the content of the magnetization component with the fast relaxation rate.

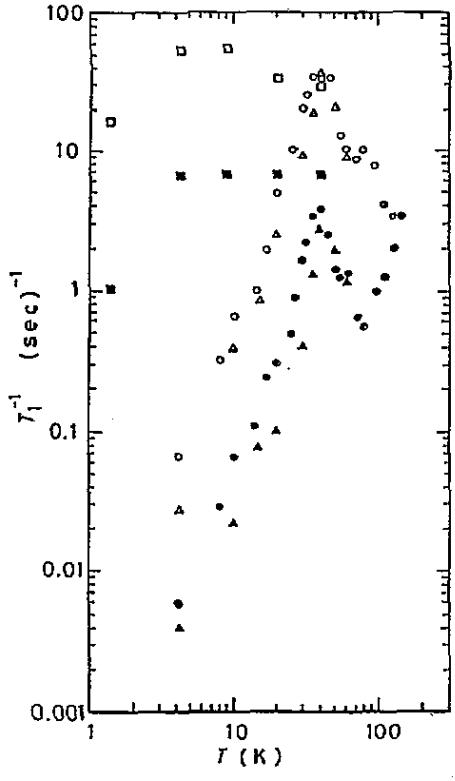

Figure 10. Temperature dependences of $(T_1^S)^{-1}$ (△, ○, □) and $(T_1^L)^{-1}$ (▲, ●, ■): △, ▲, La(I) site in $La_2NiO_{4.00}$; ○, ●, La site in $La_2NiO_{4.02}$; □, ■, La site in $La_2NiO_{4.10}$.

where M_S and M_L are the parameters appearing in equation (9). The T dependence of $(T_2^L)^{-1}$ and $(T_2^S)^{-1}$ for ^{139}La in $La_2NiO_{4.02}$ deduced through these procedures is shown in figure 11 on a log–log scale. Both $(T_2^L)^{-1}$ and $(T_2^S)^{-1}$ show complicated but similar dependences on T.

3.6. Effect of Sr substitution for La

The substitution of Sr atoms for La atoms in $La_{2-x}Sr_xNiO_{4+\delta}$ has been known to dope the holes in the system, resulting in the suppression of AF ordering.

If we assume an ionic picture of $(La^{3+})_{2-x}(Sr^{2+})_x(Ni\text{–}O)^P(O^{2-})_{3+\delta}$, the Ni–O valence P is given by $x + 2\delta$. Therefore, we plot the dependence of H_{int} on the value of P in figure 12, where the open circles show the excess oxygen doping and the full circles the Sr substitution. In the latter case, we assumed that δ was zero. As can be seen in the figure, H_{int} hardly changes in the valence range $0.04 < P < 0.7$ and then exhibits a considerable decrease at $P \simeq 1.0$ ($x \simeq 1.0$). In a previous paper [13], we reported the evolution of an NMR signal in the paramagnetic state ($H_{int} = 0$) above $P \simeq 1.0$. This provided microscopic evidence for the phase transition from

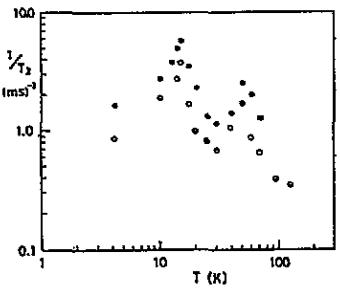

Figure 11. Temperature dependences of $(T_2^L)^{-1}$ (○) and $(T_2^S)^{-1}$ (●) for ^{139}La in $La_2NiO_{4.02}$ deduced through the procedure described in the text.

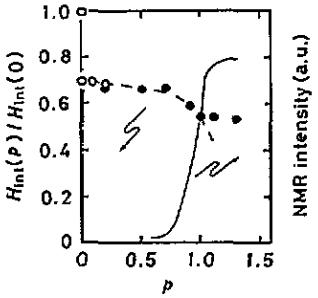

Figure 12. Dependence of H_{int} on the Ni–O valency P: ○, hole doping by the excess oxygen ($P = 2\delta$); ●, hole doping by Sr substitution ($P \simeq x$); ——, dependence of the NMR intensity on P.

the AF to the paramagnetic (metallic) state at $P \simeq 1.0$ without any intermediate superconducting phase.

4. Discussion

We have reproduced the suppression of AF ordering in $La_2NiO_{4+\delta}$ when excess oxygen atoms are introduced and also when Sr atoms are substituted for La atoms.

In the case of $La_{2-x}Sr_xCuO_4$, the destruction of antiferromagnetism at $x \simeq 0.05$ has been generally explained as follows. The doped hole is accommodated with the $2p_{x,y}$ orbital of O_{planar}. This would result in an increase in the correlation between the holes in d_{z^2} and in $2p_{x,y}$ with antiparallel spin ($S = \frac{1}{2}$), giving rise to frustration of the antiparallel Cu spin alignment.

The critical content $x \simeq 1.0$ in $La_{2-x}Sr_xNiO_4$ is, however, extremely large compared with $x \simeq 0.05$ in $La_{2-x}Sr_xCuO_4$. To explain this result, Cava *et al* [12] suggested that the doped holes primarily go into the $3d_{z^2}$ and then into the $3d_{x^2-y^2}$ orbitals in a continuous fashion, because the lattice parameter c increases up to $x \simeq 0.5$ (see figure 1). For complete understanding of the transition mechanism for $LaSrNiO_4$, however, a microscopic view of the hole distribution in Ni and the surrounding oxygen atoms is required.

In this section, we discuss possible mechanisms that produce some characteristic properties observed by ^{139}La NQR in $La_2NiO_{4+\delta}$ in comparison with the corresponding properties in La_2CuO_4.

4.1. Magnetic structure

In the AF state, the alignment of the Ni moments determined by neutron diffraction [7] is in the direction along the ⟨110⟩ axis in the basal plane. The spectrum of ^{139}La NQR in the $La_2NiO_{4.02}$ single crystal when H_{ext} is applied indicates that the direction of H_{int} at the La site is close to the ⟨110⟩ axis (angle $\theta = 77°$ with the c axis). If one takes the crystal symmetry into account, the direction of H_{int} at the La site is consistent with the alignment of the Ni moments along ⟨110⟩.

In the case of La_2CuO_4 [18,20] the experimental magnitude of H_{int} (H_{int} = 1.0 kOe; $\theta = 78°$) has been explained by the dipole field H_{dip}, originating from the Cu moments in the sublattice structure in which the magnetic moment (1 μ_B) orders antiferromagnetically in the basal plane with slight canting along the c axis (figure 13(*b*)). However, the magnetic moment of Cu^{2+} measured by neutron diffraction [22] is only about 0.5 μ_B. Thus the dipole field caused by Cu^{2+} is not sufficient to explain the experimental magnitude of H_{int} at the La site. In the case of La_2NiO_4, the experimentally large magnitude of H_{int} (H_{int} = 26.2 kOe for La(I) and 18.3 kOe for La(II); $\theta = 77°$) cannot be explained at all by the dipole field caused by the Ni^{2+} moment of 1.6 μ_B [5].

In the ionic picture of $(La^{3+})_2(Ni^{2+})(O^{2-})_4$, two holes are present in $3d_{x^2-y^2}$ and in $3d_{z^2}$ orbitals of Ni and two holes in the 6s orbital of La. The holes in both 6s and $3d_{z^2}$ will migrate to the $2p_z$ orbital of O_{apex}. Recently, Takahashi *et al* [23] reproduced theoretically the experimental magnitude of H_{int} in La_2NiO_4 by a cluster model calculation, where the interference of the migration of the holes in 6s and $3d_{z^2}$ with parallel spin to $2p_z$ is shown to be mainly responsible for the superhyperfine interaction, giving rise to the relatively strong H_{int} at the La site.

As can be seen in figure 6, at the La(I) site in $La_2NiO_{4.00}$, $\nu_M(T)/\nu_M(0)$ (and, therefore, H_{int}), shows a discontinuous increase of about 1.6% at about 80 K. The x-ray diffraction shows that, at the structural phase transition from LTO_2 to LTO_1 near 75 K, the lattice parameter c changes continuously but the parameters *a* and *b* vary, with roughly a mean value of the parameters *a* and *b* with decreasing *T*. Thus the discontinuity in H_{int} is associated with the change in the parameter *a* (*b*). This gives us important information that H_{int} *in a phase close to tetragonal is smaller than that in the orthorhombic phase.*

For the sample with $\delta = 0.02$, the width of the main resonance lines significantly broadens below 25 K, corresponding to the sharp peak in $\chi(T)$ at about 20 K. This result suggests the existence of magnetic ordering below about 20 K, the weak ferromagnetism along the *c* axis probably arising from the slight canting of the spins (see figure 13(*a*)).

4.2. Introduction of excess oxygen

We have shown that a somewhat complex ^{139}La resonance spectrum appeared when the content of excess oxygen increased from $\delta = 0.00$ to 0.10 and could be reproduced by the spectrum given by one of three parameter sets (H_{int} = 26.2 kOe; ν_Q = 8.7 MHz), (H_{int} = 18.3 kOe; ν_Q = 4.0 MHz) and (H_{int} = 17.8 kOe; ν_Q = 2.6 MHz), or by superposition of the spectra.

The NQR spectrum for $La_2NiO_{4.00}$ at 1.4 K shown in figure 3(*a*) indicates the existence of two inequivalent La sites with comparable contents: the La(I) site with H_{int} = 26.2 kOe and ν_Q = 8.7 MHz and the La(II) site with H_{int} = 18.3 kOe and ν_Q = 4.0 MHz. As the profile of the spectrum does not change up to $T \simeq 200$ K, the appearance of the two inequivalent sites does not correlate with the structural phase transition from LTO_1 to LTO_2 at 75 K. The x-ray pattern at room temperature indicates that the sample is in a well characterized single orthorhombic phase. Thus, for the La(I) and La(II) sites in $La_2NiO_{4.00}$, we cannot find any difference in the crystal symmetries or in the lattice parameters.

The discretization of the H_{int} and ν_Q magnitudes obtained from the ^{139}La NQR spectra suggests that there are some specified contents δ_{sp} at around 0.00, 0.02 and 0.1 where the accommodation of the excess oxygen is stable, probably forming

superlattices of the interstitial oxygen atoms. The appearance of the two inequivalent La sites in $La_2NiO_{4.00}$ could be understood if the sample were composed of two parts in the microscopic region with $\delta_{sp} \simeq 0.00$ for La(I) and $\delta_{sp} \simeq 0.02$ for La(II).

H_{int} and ν_Q exhibit a sudden decrease on increase in δ_{sp} from 0.00 to about 0.02. This H_{int} discontinuity is considered to be attributed to the structural change from LTO_1 to HTT with the introduction of excess oxygen because, as we have indicated in section 4.1, H_{int} in the LTO_2 phase close to the tetragonal phase is smaller than in the LTO_1 phase. Gopalan *et al* [8] observed a similar discontinuity in T_N at $\delta \simeq 0.005$. They suggested the possibility that the T_N discontinuity correlates with the decrease in orthorhombicity with increasing δ. The interstitial accommodation or the lack of oxygen requires local lattice distortion, giving rise to a distortion of the NiO_6 units [24]. This would significantly change the Ni–O_{apex}–La superhyperfine interactions.

4.3. Sr substitution for La

Destruction of the antiferromagnetism and the appearance of the non-magnetic metal phase occur at the large Sr content $x \simeq 1.0$. The magnitude of H_{int} remains almost constant in the region $0.04 < P \lesssim 0.7$, where P denotes the Ni–O valency. The extremely large critical Sr content in $La_{2-x}Sr_xNiO_{4+\delta}$ in contrast with that in $La_{2-x}Sr_xCuO_4$ might be possible if the doped holes go first into Ni $3d_{z^2}$ up to $P \simeq 0.5$ [12] and then into $3d_{x^2-y^2}$; the latter would induce spin frustrations of Ni at large P. If this is the case, we can expect some variations in H_{int} in the range $x = 0$–0.5, following the theory of Takahashi *et al* [23]. The increase in the up-spin hole occupation in $3d_{z^2}$ should increase the hole transfer to $2p_z$ of O_{apex}, counteracting the up-spin hole transfer from La 6s to $2p_z$. Thus, in the La 6s orbit, the difference between the amounts of up- and down-spin occupation is considered to increase, resulting in an increase in H_{int}. This disagrees with the experimental result.

Thus *the H_{int} plateau up to $P \simeq 0.7$ leads to the conclusion that the doped holes primarily go into the $3d_{x^2-y^2}$ orbital.* Igarashi [25] suggested that the doped holes possibly go into $3d_{x^2-y^2}$ without producing spin frustrations of Ni. The reason is as follows. The doped holes accommodated in $2p_{x,y}$ of O_{planar} increase the correlation between the holes in $d_{x^2-y^2}$ and in $p_{x,y}$ with antiparallel spins, as in the case of $La_{2-x}Sr_xCuO_4$. However, because of the large number of Ni spins ($S = 1$), the AF superexchange interaction between the Ni spins can still remain.

4.4. Frequency shift of the resonance line by H_{ext} in the orthorhombic phase

The splitting of the resonance line (figure 4(*a*)) when H_{ext} is applied along ⟨110⟩ of the single crystal is analysed as indicative of the AF ordering axis being in the direction along ⟨110⟩. The magnitude of the frequency shift (0.10 MHz kOe^{-1}) caused by H_{ext} is, however, very small compared with the value of γ_N (= 0.601 MHz kOe^{-1}) for ^{139}La. The resonance frequencies of the split lines will be given as follows [26]:

$$\nu_1 = (\gamma_N/2\pi)|A_0M_1 - H_{ext}| \tag{12}$$

$$\nu_2 = (\gamma_N/2\pi)|A_0M_2 + H_{ext}| \tag{12'}$$

where $M_1 = M_2$ is the local magnetization, A_0 is the hyperfine interaction constant and the magnetic dipole field is neglected. When non-zero parallel susceptibility $\chi_\parallel$ of the antiferromagnet is allowed for, then the local magnetizations are given by

$$M_1 = M_0 + \chi_\parallel H_{ext}/2 \qquad M_2 = M_0 - \chi_\parallel H_{ext}/2 \tag{13}$$

respectively. Gopalan *et al* [8] observed the parallel susceptibilities in $La_2NiO_{4.000}$ below 650 K. The magnetic moment induced by H_{ext} may occasionally reduce the frequency shift of the resonance line.

4.5. Temperature dependence of H_{int}

In the case of La_2CuO_4 [18] the dependence of the resonance frequency on T was in accord with the prediction of spin fluctuation theory for weak itinerant antiferromagnets given by [27]

$$\nu_M(T)/\nu_M(0) = [1-(T/T_N)^{3/2}]^{1/2}. \tag{14}$$

We could not, however, reproduce the experimental data for $La_2NiO_{4.02}$ even if we took the value of T_N as a free adjustable parameter.

Then we replotted the experimental data for La(II) in the form $1-\nu_M(T)/\nu_M(0)$ ($\simeq 1-H_{int}(T)/H_{int}(0)$) in figure 14 on a log–log scale. All the data are on a straight line and, therefore, proportional to $T^{2.3}$. The extrapolation of the line reaches a value of $1-H_{int}(T)/H_{int}(0) = 1$ at $T \simeq 500$ K, giving rise to an estimate of the Néel temperature T_N.

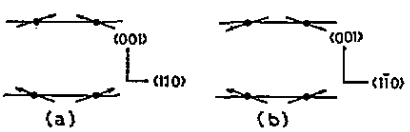

Figure 13. Model of spin structures in (*a*) La_2NiO_4 and (*b*) La_2CuO_4 obtained by Brill *et al* [21].

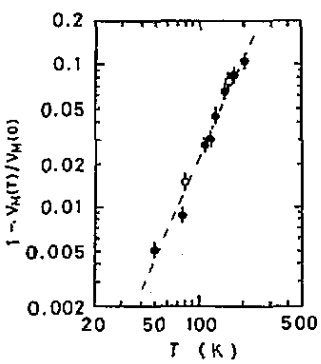

Figure 14. Plot of $1-\nu_M(T)/\nu_M(0)$ on a log–log scale: ○, La(II) in $La_2NiO_{4.00}$; ●, La in $La_2NiO_{4.02}$.

The spin-wave theory for a three-dimensional AF system [28] predicts that $1-H_{int}(T)/H_{int}(0)$ is proportional to T^2. This is not too far away from the experimental dependence of $T^{2.3}$ for $La_2NiO_{4+\delta}$ ($\delta < 0.02$). Thus *sublattice magnetic moments of Ni^{2+} exhibit a behaviour close to the localized spins, rather than the itinerant behaviour of Cu^{2+} in La_2CuO_4* [18].

4.6. Temperature dependence of T_1

As shown in figure 10, the ^{139}La relaxation rates T_1^{-1} for both La(I) and La(II) are proportional to $T^{2.6}$ below about 20 K. This temperature dependence is close to the theoretical prediction of T^3 based on the spin-wave model for the three-dimensional AF system [28].

Recently, Chakravarty *et al* [29] calculated T_1^{-1} in the quasi-two-dimensional antiferromagnet La_2CuO_4, paying particular attention to the form factors associated with different nuclear sites. If we define $\Delta = 2S\sqrt{JJ'}$, a scale of the crossover between two- and three-dimensional behaviour (J and J' are the inter-planar and intra-planar couplings, respectively), the T_1^{-1}-values in the two-dimensional regime $T_N \gg T \gg \Delta$ are given by

$$1/T_1^{Cu} \sim (aT/\hbar c)T/\Delta \tag{15}$$

$$1/T_1^{La} \sim A'(aT/\hbar c)^4 \ln(T/\Delta) + B'(aT/\hbar c)^2 T/\Delta \tag{16}$$

and in the three-dimensional regime $T < \Delta$ by

$$1/T_1^{Cu} \sim (aT/\hbar c)(T/\Delta)^2 \tag{17}$$

$$1/T_1^{La} \sim A''(aT/\hbar c)^4 (T/\Delta)^3 + B''(aT/\hbar c)^2 (T/\Delta)^3 \tag{18}$$

with $B'/A' \simeq B''/A'' \ll 1$. Hence, c is the $T = 0$ two-dimensional spin-wave velocity and a is the lattice spacing. $\Delta \simeq 20$ K for La_2CuO_4. The different behaviours of $1/T_1^{Cu}$ and $1/T_1^{La}$ arise because, at the La sites, the short-wavelength fluctuations with $Q = (\pi/a, \pi/a, 0)$ would be almost filtered owing to the geometrical cancellation.

In the case of $La_2NiO_{4+\delta}$, if we take $J \simeq 20$ meV and $J' \simeq 1.1$ meV [30], Δ is estimated to be about 100 K, being much higher than for La_2CuO_4. Thus the low-temperature $1/T_1$ data are in the three-dimensional regime. The $T^{2.6}$ dependence observed experimentally is far from T^{5-7} dependence given by equation (18) but close to T^3 dependence given by equation (17). So we must conclude that *the observed relaxation can be ascribed to the short-wavelength fluctuations.* This may be plausible in $La_2NiO_{4+\delta}$ because approximately one hole occupies Ni $3d_{z^2}$ which is hybridized with $2p_z$ of O_{apex}, providing a strong La relaxation channel.

As for the magnitude of the relaxation rate, T_1^{-1} is expected here to be proportional to H_{int}^2. This disagrees with the experimental result that T_1^{-1} at La(I) ($H_{int} = 26.2$ kOe) is smaller than T_1^{-1} at La(II) ($H_{int} = 18.2$ kOe). In addition, the experimental magnetization recovery gives at least two relaxation rates, namely $(T_1^S)^{-1}$ and $(T_1^L)^{-1}$, for each of the La sites with the same H_{int}. Thus, one must take the other parameters that control the magnitude of $1/T_1^{La}$ into account, such as the local change in the value of Δ.

On the other hand, as shown in figure 10, T_1^{-1} shows a broad bump at about 40 K for both La(I) and La(II) sites. A similar enhancement in T_1^{-1} was observed in La_2CuO_4 at about 7 K [31]. One cannot attribute it to quadrupole relaxation caused by lattice instabilities associated with the LTO_2-to-LTO_1 phase transition, because the phase transition at the La(I) site does not occur at the La(II) site in $La_2NiO_{4.02}$. It is also difficult to attribute it to the other possible structural fluctuations, because it should be effective at different T-values for La(I) and La(II) observed at the different resonance frequencies 11.7 and 18 MHz.

Contrary to the strongly T-dependent T_1^{-1} in the deoxygenated samples, T_1^{-1} in oxygenated $La_2NiO_{4.10}$ is almost independent of T and very large. It has been suggested that the highly oxygenated sample contains a considerable amount of Ni^{3+} ions. The T-independent T_1^{-1} would, therefore, be associated with Ni^{3+} spin fluctuations caused by possible exchange couplings between the Ni^{3+} spins.

As a final conclusion, our study shows that, even if the ^{139}La NQR behaviour of the La_2NiO_4 system is highly complex, some marked differences from the La_2CuO_4 system exist, originating from the difference in the hole and spin numbers.

(1) The large internal magnetic field at the La site is controlled by interference in the migration of a second hole of Ni in $3d_{z^2}$ and a hole in La 6s with the parallel spin on $2p_z$ of O_{apex}.

(2) The strong discontinuity in H_{int} and EFG at $\delta \simeq 0.02$ is attributed to the LTO-to-HTT crystal phase transition.

(3) H_{int} remains almost constant for Sr substitution up to $x \simeq 0.7$, in support of the idea that the doped holes go first into the Ni $3d_{z^2}$ orbital without producing Ni–Ni spin frustrations.

(4) The T dependences of H_{int} and T_1^{-1} at low T are explained basically by the spin-wave theory for three-dimensional antiferromagnets and, therefore, the sublattice magnetic moments of Ni^{2+} are close to the localized spins.

(5) The low-temperature T_1^{-1} proportional to $T^{2.6}$ indicates that the ^{139}La relaxation is attributed significantly to the short-wavelength AF fluctuations notwithstanding the geometrical cancellation at the La site.

References

[1] Buttrey D J, Honig J M and Rao C N 1986 *J. Solid State Chem.* **64** 287

[2] Honig J M and Buttrey D J 1985 *Localization and Metal Insulator Transitions* ed H Fritzche and D Adler (New York: Plenum) p 409

[3] Tavaves C P 1985 *Mat. Res. Bull.* **20** 979

[4] Rodriguez-Carvajal J, Matinez J L, Pannetier J and Saez-Puche R 1988 *Phys. Rev.* B **38** 7148

[5] Lander G H, Brown P J, Spalek J and Honig J M 1989 *Phys. Rev.* B **40** 4463

[6] Nanjundaswami K S, Lewicki A, Kakol Z, Gopalan P, Metcalf P, Honig J M, Rao C N R and Spalek J 1990 *Physica* C **166** 361

[7] Aeppli G and Buttrey D J 1988 *Phys. Rev. Lett.* **61** 203

[8] Gopalan P, McElfresh M W, Kakol Z, Spalek J and Honig J M 1992 *Phys. Rev.* **45** 249

[9] Kajitani T, Kitagaki Y, Hiraga K, Hosoya S, Fukuda T, Yamaguchi Y, Wada S, Sugai S, Morii Y, Fuchizaki K and Funahashi S 1991 *Physica* C **185–9** 579

[10] Schirber J E, Venturini E L, Morosin B, Kwak J F, Ginley D S and Banghman R J 1987 *High-temperature Superconductors II (Mater. Res. Soc. Symp. Proc. 99)* ed M B Brodsky, R C Dynes, K Kitazawa and H L Taller (Pittsburgh, PA: Material Research Society) p 470

[11] Tholence J L 1987 *Physica* B **148** 353

[12] Cava R J, Batlogg B, Palstra T T, Krajewski J J, Peck W F Jr, Ramirez A P and Rupp L W Jr 1991 *Phys. Rev.* B **43** 1229

[13] Furukawa Y and Wada S 1992 *J. Phys. Soc. Japan* **61** 1182

[14] Wada S, Kobayashi T, Kaburagi M, Shibutani K and Ogawa R 1989 *J. Phys. Soc. Japan* **58** 2658

[15] Wada S, Kobayashi T, Kaburagi M, Kajitani T, Hosoya S, Fukuda T, Onodera S, Yamada Y, Shibutani K and Ogawa R 1990 *Physica* B **165–6** 1313

[16] Das T P and Hahn E L 1958 *Solid State Physics* Suppl 1, ed F Seitz and D Turnbull (New York: Academic)

[17] In our previous papers [14,15] we presented a set of parameters given by $\nu_Q = 1.8$ MHz, $H_{int} = 19.3$ kOe and $\theta \simeq 5°$, which also reproduces the experimental spectrum for $\delta = 0.02$. In the present experiment for the single crystal, however, we confirmed that the axis of V_{zz} is in the direction along the c axis, and the polar angle ($\theta \simeq 5°$) of H_{int} with respect to V_{zz} opposes the AF ordering axis and is in the direction along ⟨110⟩.

[18] Nishihara H, Yasuoka H, Shimizu T, Tsuda T, Imai T, Sasaki S, Kambe S, Kishio K, Kitazawa K and Fueki K 1987 *J. Phys. Soc. Japan* **56** 4559

[19] Narath A 1967 *Phys. Rev.* **162** 320

[20] Kitaoka Y, Hiramatsu S, Kohara T, Asayama K, Oh-ishi K, Kikuchi M and Kobayashi N 1987 *Japan. J. Appl. Phys.* **26** L397

[21] Brill T M, Hampel G, Mertens F, Schurmann R, Assmus W and Luthi B 1991 *Phys. Rev.* B **43** 10548

[22] Freltoft T, Fisher J E, Shirane G, Moncton D E, Sinha S K, Vaknin D, Remeika J P, Cooper A S and Harshman D 1987 *Phys. Rev.* B **36** 826

[23] Takahashi M, Nishino T and Kanamori J 1991 *J. Phys. Soc. Japan* **60** 1365
[24] Jorgensen J D, Dabrowski B, Pei S, Hinks D G, Soderholm L, Morosin B, Schirber J E, Venturini E L and Ginley D S 1988 *Phys. Rev.* B **38** 7148
Jorgensen J D, Dabrowski B, Pei S, Richards D R and Hinks D G 1989 *Phys. Rev.* B **40** 2187
[25] Igarashi J 1991 private communication
[26] Turov E A and Petrov M P 1972 *Nuclear Magnetic Resonance in Ferro- and Antiferromagnets* (New York: Wiley)
[27] Hasegawa H and Moriya T 1978 *J. Phys. Soc. Japan* **36** 1542
[28] Moriya T 1956 *Progr. Theor. Phys.* **16** 641
[29] Chakravarty S, Gelfand M P, Kopietz P, Orbach R and Wollensak M 1991 *Phys. Rev.* B **43** 2796
[30] Axe D, Moudden H, Holhwein D, Cox D E, Mohanty K M, Moodenbaugh A R and Xu Y 1989 *Phys. Rev. Lett.* **62** 2571
[31] Sasaki S, Yasuoka H, Shimizu T, Nishihara H, Tsuda T, Sugii N, Kambe S, Kishio K, Kitazawa K and Fueki K 1988 *J. Phys. Soc. Japan* **57** 1151